A

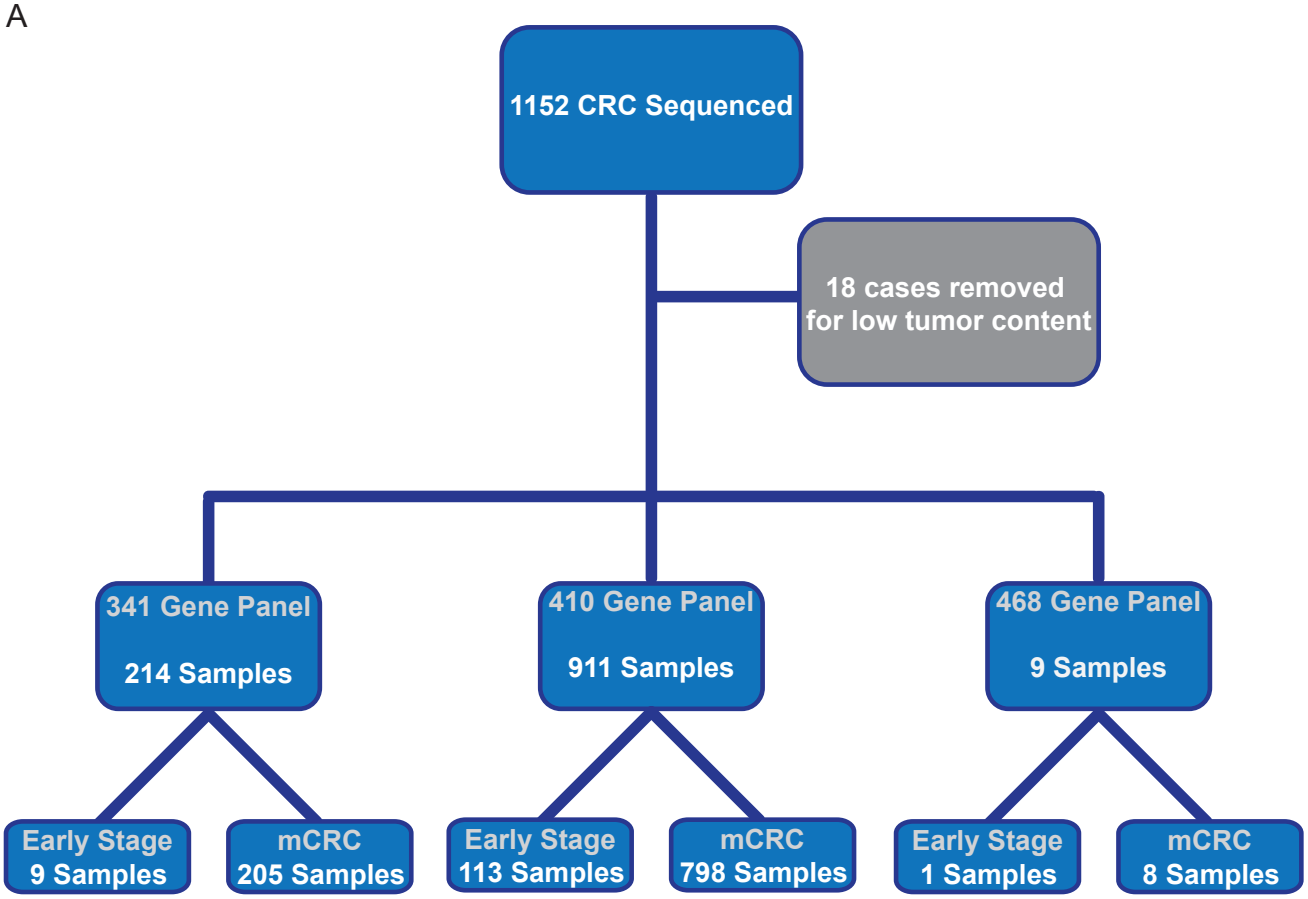

B

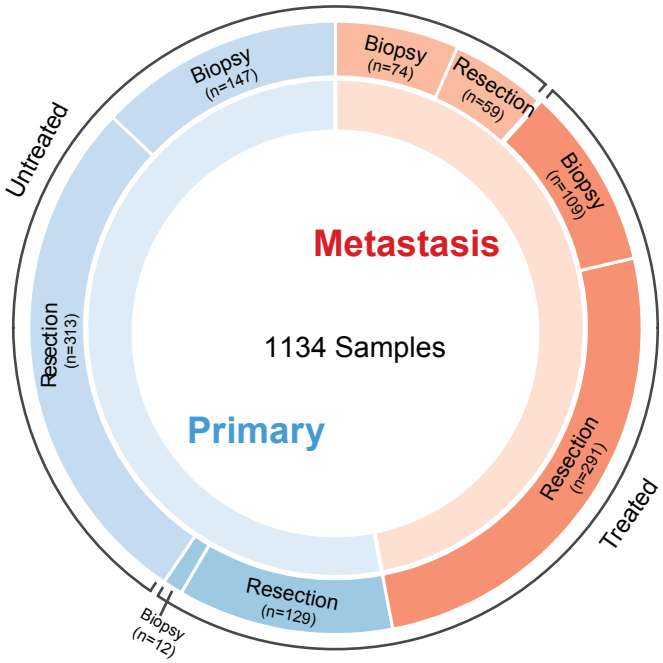

Figure S1, related to Table 1.
(A) Sample flow diagram illustrating samples analyzed. (B) Pie chart showing sample characteristics.

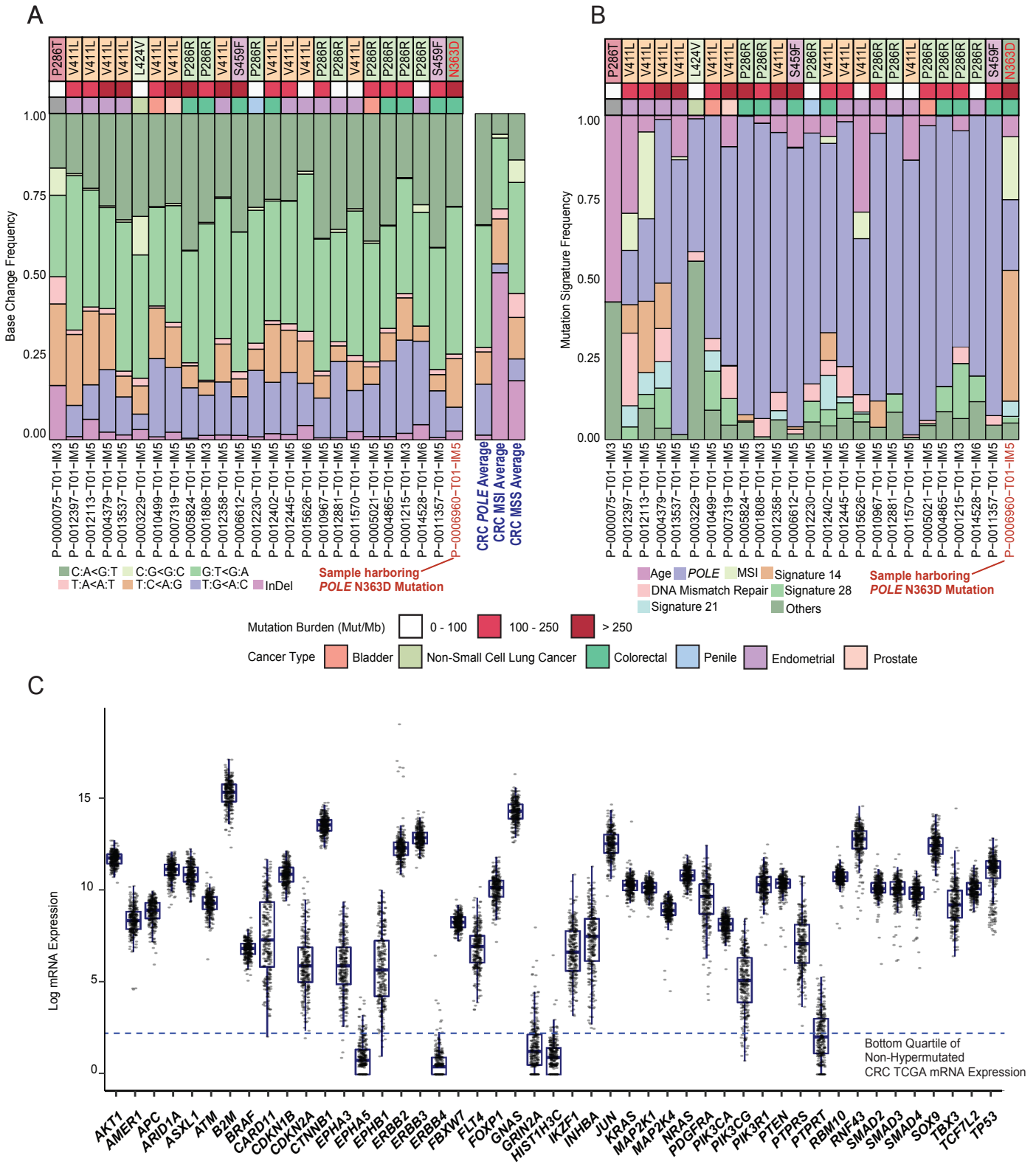

Figure S2, related to Figure 1.

(A) Spectrum of nucleotide base changes in all ultra-mutated *POLE* mutant tumors analyzed with MSK-IMPACT. (B) Mutational signatures in all ultra-mutated *POLE* mutant tumors analyzed with MSK-IMPACT. (C) mRNA expression of 47 significantly recurrently mutated genes identified in our cohort within TCGA non-hypermutated CRC cases. The line in the boxes correspond to the median. The top and bottom of the boxes correspond to the third and first quartiles, respectively. The lines above and below the box correspond to the largest and smallest non-outlier values. Data points above or below the limits are considered outliers.

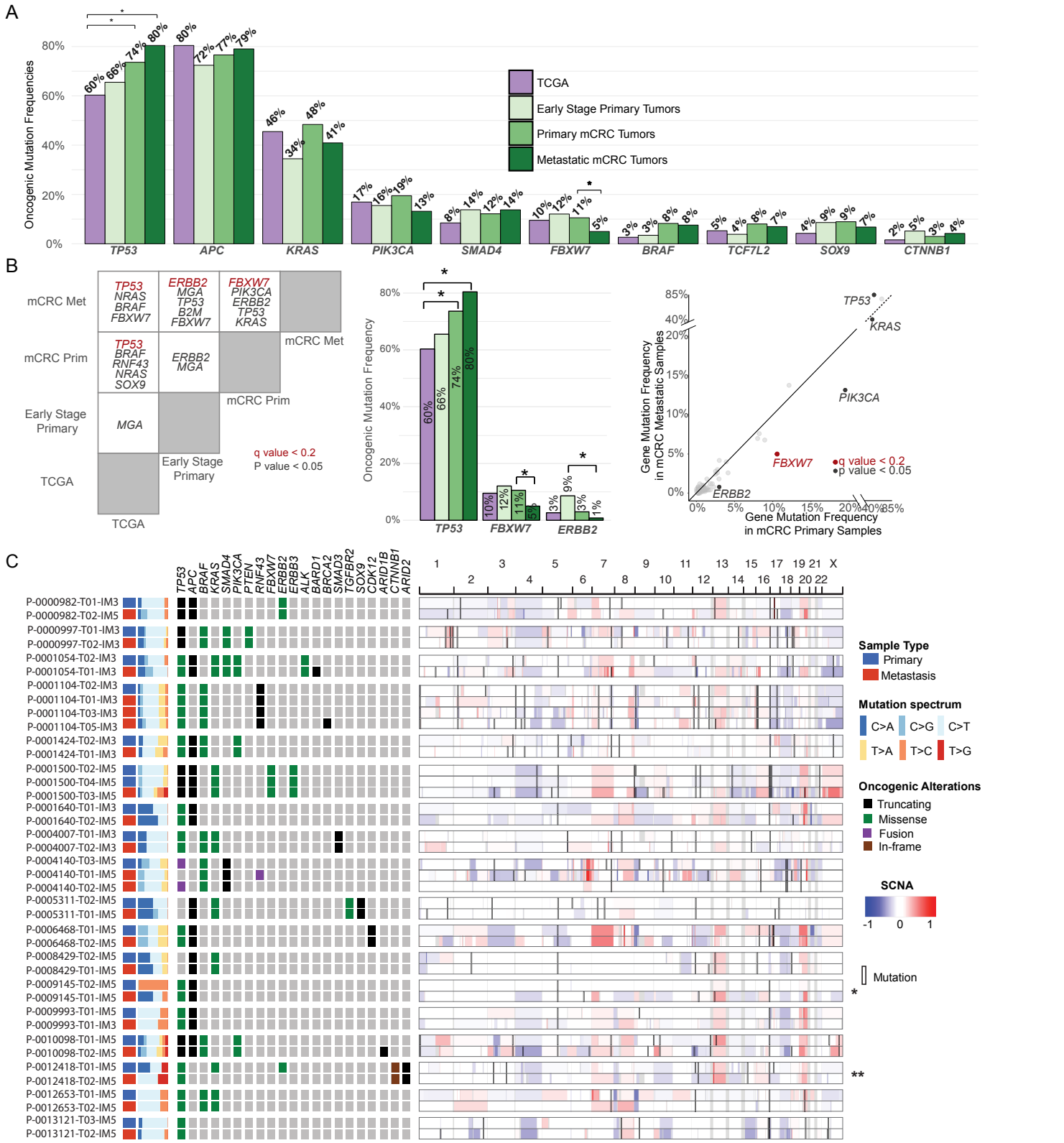

Figure S3, related to Figure 1.

(A) Significant differences in oncogenic mutations in four progressively advanced disease states: TCGA primary tumors, early stage primary tumors analyzed by MSK-IMPACT, primary tumors from patients with mCRC, and metastatic tumors. (B) Enrichment analysis for genomic alterations that significantly differ between primary tumors and metastases from patients with mCRC. (C) Spectrum of genomic alterations detected in cases with multiple samples available from the same patient for sequencing. The two significant differences in genomic alterations detected are marked with stars (*) and consisted of one case with fewer copy number alterations in the primary tumor that appeared artifactual due to low tumor content in this specimen and one case with subclonal *KRAS* G13C and *ERBB2* V777L mutations detected at variant allelic frequencies of 3.5% and 7%, respectively, in the primary that were not present in the metastasis, suggesting early branching of the metastatic clone in this tumor.

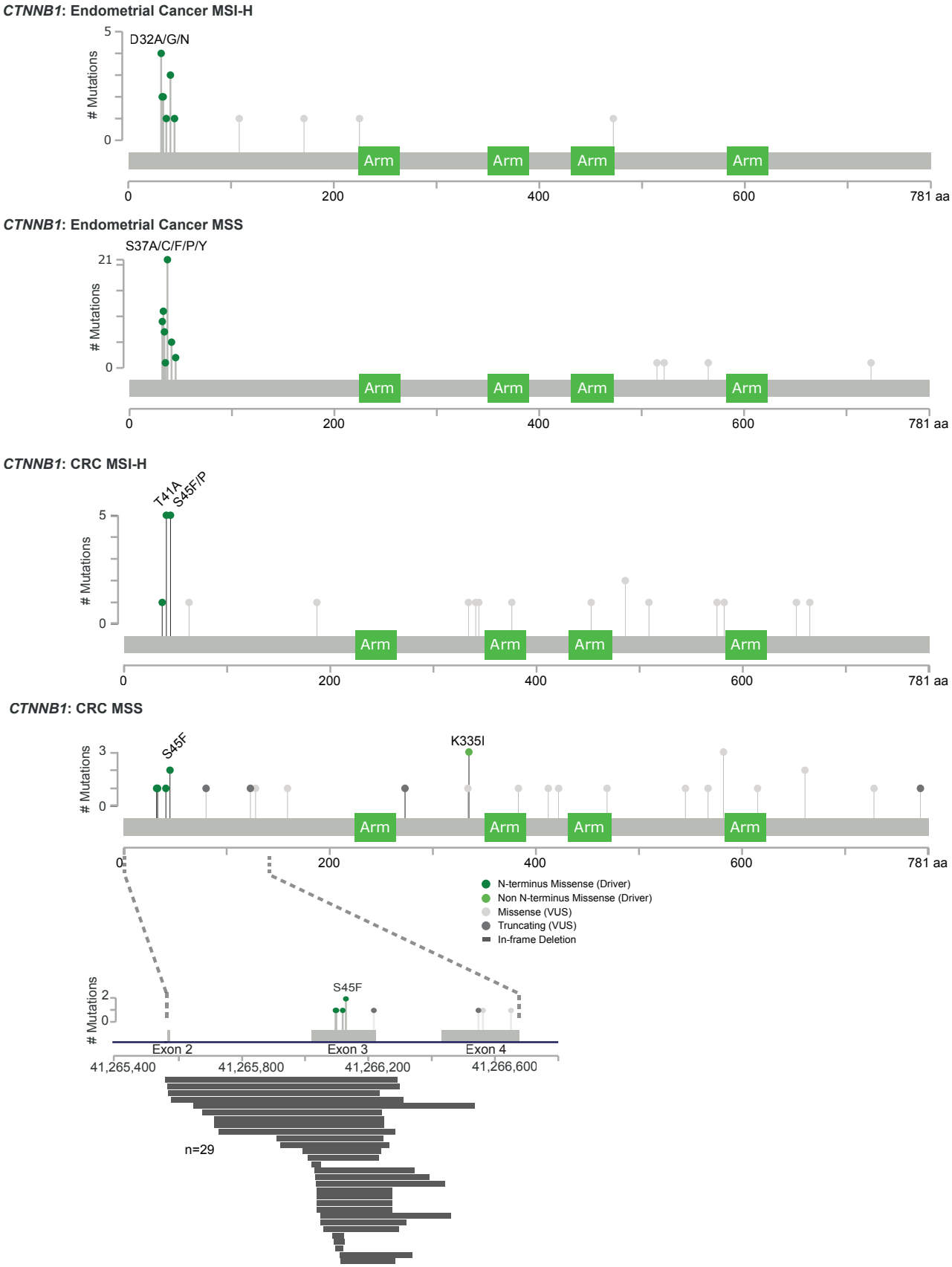

Figure S4, related to Figure 2.
The spectrum of *CTNNB1* alterations in endometrial cancer and MSI-H and MSS CRC. The plots related to CRC are identical to those seen in Figure 2C. They are shown for the purpose of easier comparison to endometrial cancer.

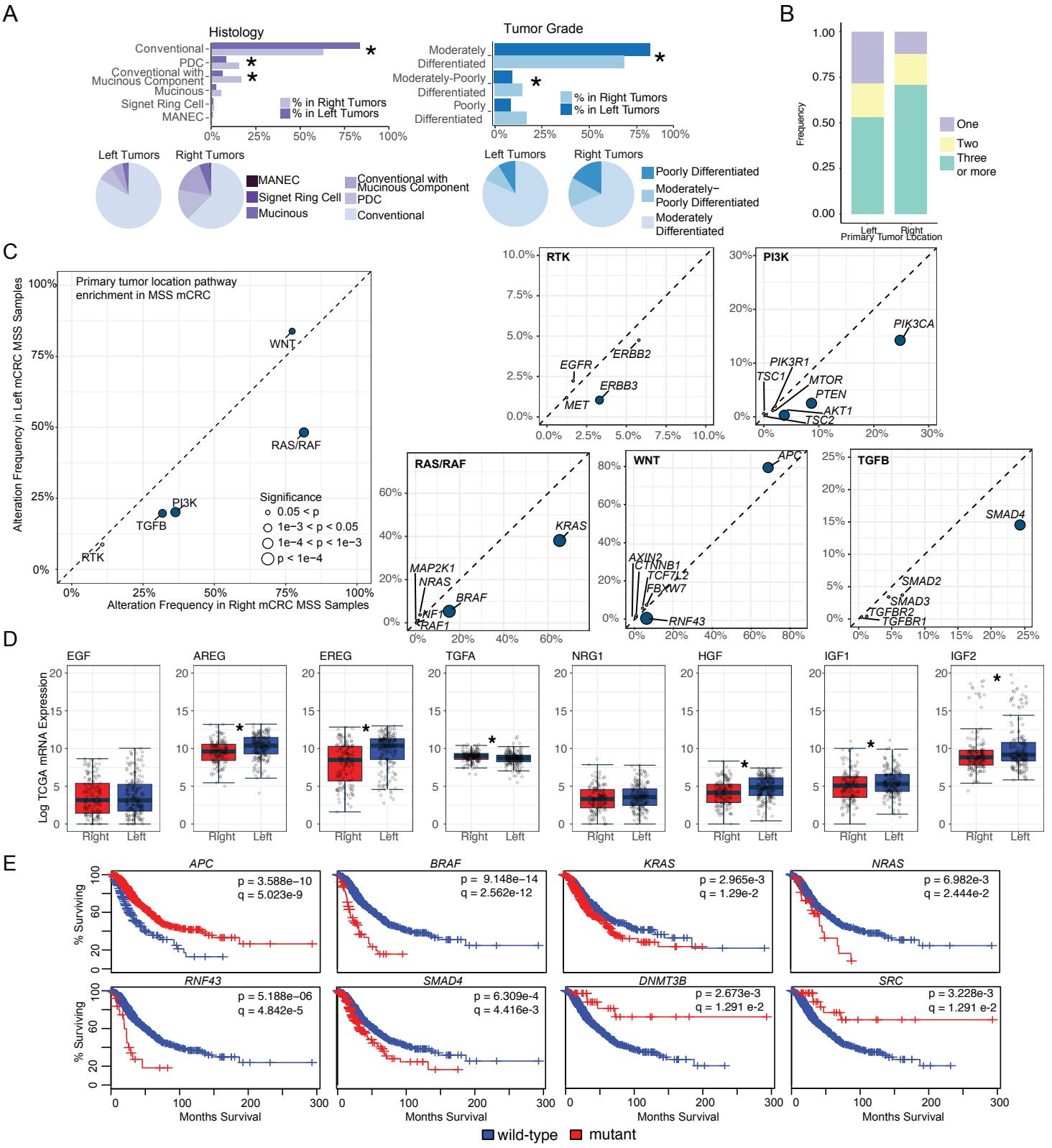

Figure S5, related to Figure 4.

(A) Histology and grade of primary tumors by tumor site. (PDC-poorly differentiated carcinoma, MANEC-mixed adenoneuroendocrine carcinoma) (B) Number of metastatic sites involved at time of diagnosis of metastases by primary tumor site in MSS metastatic CRC. (C) Pathway enrichment analysis by primary tumor site in MSS metastatic CRC cases. (D) Analysis of ligand expression in TCGA samples by primary tumor site. Star (*) indicates statistically significant difference at p<0.05 level. The line in the boxes correspond to the median. The top and bottom of the boxes correspond to the third and first quartiles, respectively. The lines above and below the box correspond to the largest and smallest non-outlier values. Data points above or below the limits are considered outliers. (E) Kaplan-Meier curves for genes in MSK-IMPACT with significant effect on OS after filtering for genes with at least 20 cases of oncogenic alterations in our series.

A

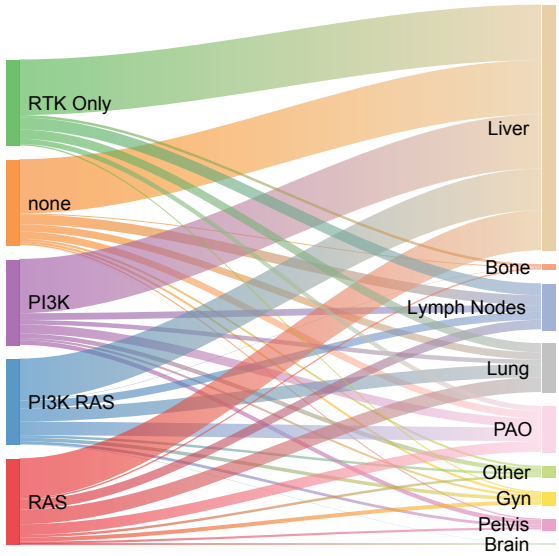

Metastatic Site	Pathway Group	% of this group	% other groups	p value
Liver	None	78%	71%	0.01963
	RAS	69%	76%	0.0082
	RTK ONLY	86%	73%	0.04649
Lung	None	10%	22%	2.29E-05
	PI3K	7%	19%	0.0101
	RAS	25%	14%	1.54E-05
PAO	None	11%	18%	0.002559
	PI3K RAS	23%	14%	0.01016

B

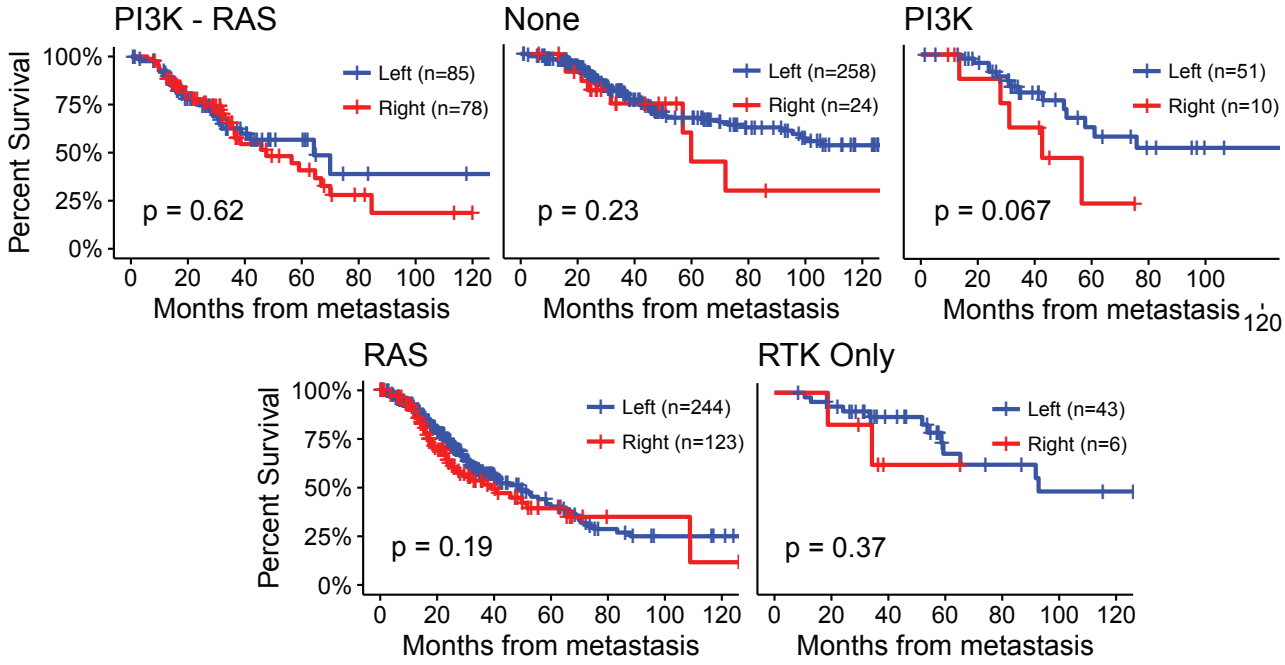

Figure S6, related to Figure 5.
(A) Sankey diagram (top) illustrating relative flow of first site of metastasis from each of the molecular pathway subgroups. (Gyn refers to ovaries, fallopian tubes, uterus, cervix, and vagina; PAO refers to peritoneum, abdominal wall or omentum) Bottom panel lists sites with significant differences in involvement by molecular pathway subgroups. (B) Kaplan-Meier curves for OS from time of diagnosis of metastatic disease by tumor laterality in each of the five genomic subgroups.